Present and Future of Modeling Global Environmental Change: Toward Integrated Modeling, Eds., T. Matsuno and H. Kida, pp. 77–87.

Effects of Man-Made Air Pollution on the Climate

Teruyuki NAKAJIMA[1], Akiko HIGURASHI[2], Kazuaki KAWAMOTO[3] and Toshihiko TAKEMURA[1]

[1]*Center for Climate System Research, The University of Tokyo, 4-6-1 Komaba, Meguro-ku, Tokyo 153-8904, Japan*
[2]*National Institute for Environmental Studies, 16-2 Onogawa, Tsukuba, Ibaraki 305-0053, Japan*
[3]*Virginia Polytechnic Institute and State University, also at NASA Langley Research Center, Atmospheric Sciences Division, Mail Stop 420 Hamptom, VA 23681, U.S.A.*

INTRODUCTION

Anthropogenic aerosols generated from global scale air pollution have been drawing recent intensive attention from the climate study community. One of the significant effects of man-made air pollution is its generation of fine aerosol particles, which further cause an earth's climate change through various processes as aerosol direct radiative effect, indirect radiative effect, and precipitation change (Charlson *et al*., 1992; Rosenfeld, 2000). The direct effect of aerosols is that aerosols directly scatter and absorb the radiation, while the indirect effect is caused by aerosols acting as cloud condensation nuclei (CCN) to change the cloud lifetime. Even with the intensive past studies as in the IPCC (Intergovernmental Panel of Climate Change) studies (e.g., IPCC95, 1996), large uncertainty still remains for the evaluated values of aerosol radiative forcing.

Table 1 summarizes the past studies of radiative forcing caused by anthropogenic climate change factors after the industrial revolution. The total forcing of trace gases is well estimated to be +2.4 W/m^2 including the effect of greenhouse gas increase and ozone change. The uncertainty is about –0.3 W/m^2. Forcing of the aerosol direct effect is about –0.4 W/m^2, but the uncertainty is larger than 0.3 W/m^2. This uncertainty is caused by the difference in the assumed aerosol concentration, vertical profile and chemical structure for the evaluation. Indirect forcing is hardly been studied because of the complicated processes involved. Two major mechanisms have been recognized. The first kind is the indirect effect caused by an increase in the optical thickness of the cloud layer with decreasing cloud droplet size when aerosol particles act as CCN. The second kind is the indirect effect caused by a liquid water path change when the cloud lifetime changes with the increasing CCN. Table 1 shows a few estimates from the limited studies ranging from –0.7 W/m^2 to –1.7 W/m^2 with a large uncertainty of 1 W/m^2.

Table 1. Some estimates of the radiative forcing of various anthropogenic factors after the industrial revolution in W/m^2.

Reference /Factor	Charlson *et al.* (1987)	IPCC94 (1994)	IPCC95 (1996)	Hansen *et al.* (1998)	Takemura *et al.* (2001)	Nakajima *et al.* (2001)
GHGs (CO_2, CH_4, N_2O, CFCs)	—	+2.4 ± 0.3	+2.4 ± 0.3	+2.3 ± 0.3	—	—
Strato. O_3	—	–0.1 ± 0.1	–0.1 ± 0.1	–0.2 ± 0.1	—	—
Tropo. O_3	—	+0.4 ± 0.2	+0.4 ± 0.2	+0.4 ± 0.2	—	—
Tropo. aerosols						
Direct effect (components)	–1.3	–0.9 ± 0.6	–0.5 ± 0.7	–0.4 ± 0.3	–0.19	—
Fossil fuel					–0.18	—
Sulfate	–1.3	—	–0.4 ± 0.3	—	–0.32	—
OC	—	—	—	—	–0.05	—
BC	—	—	+0.1 ± 0.1	—	+0.19	—
Biomass bng.	—	—	–0.2 ± 0.3	—	–0.01	—
OC	—	—	—	—	–0.16	—
BC	—	—	—	—	+0.15	—
Indirect effect	–1.0	–0.9 ± 0.7	–0.7 ± 0.7	–1.0–1.0+0.5	—	–0.7~–1.7
Others	—	+0.3 ± 0.2	+0.3 ± 0.2	+0.2 ± 0.4	—	—

In order to improve our knowledge of the radiative forcing of aerosols, a large effort started to be invested in studies of climate modeling, satellite remote sensing and in situ measurements. In this paper, I like to review some of such efforts in our group.

REMOTE SENSING OF AEROSOLS AND CLOUDS

Visible and infrared passive remote sensing is one of new technologies for studying the direct and indirect effects of aerosols. Aerosol optical thickness, cloud optical thickness and the effective radius of cloud droplets are among these important retrieval parameters. The characteristics changes in these parameters provide evidences of the large-scale signatures of cloud-aerosol interactions (e.g., Platnick *et al*., 2000).

The two channel method of Higurashi and Nakajima (1999) has been successfully applied to satellite image data to obtain global distributions of aerosol optical thickness, τ_α, and Ångström exponent, α, when the spectral optical thickness is fit by the Ångström's law (Nakajima and Higurashi, 1998; Higurashi *et al*., 2000),

$$\tau_\lambda = \tau_\alpha \left(\lambda / \lambda_0 \right)^{-\alpha} \tag{1}$$

where λ_0 is the reference wavelength. We adopt in this study λ_0 = 0.5 μm. As known by light scattering theory, a large Ångström exponent suggests that small particles dominate in the aerosol polydispersion. Figure 1 shows the monthly mean global distributions of the Ångström parameters for January and July 1990. It is found that τ_α is as large as 0.5 over the subtropical Atlantic Ocean off the Saharan region. This is caused by soil dust particles from the Saharan desert as discussed intensively by several investigators (Herman *et al*., 1997; Moulin *et al*., 1997). Outflows of dust particles from other arid regions, such as the Middle Asian deserts to the Arabian Sea region in July, are also distinct due to their large optical thickness and small Ångström exponent. The tropical region is characterized by a large Ångström exponent suggesting the dominance of small particles, such as in Indonesia, off Peru, and South African regions. Biomass burning aerosols will be the main component of such small particle aerosols. It is found from the figure that these small particles are collected by the tropical convergence wind system to form a tropical belt of small particles surrounding the globe, as revealed by the large Ångström exponent belt at equator. Industrial aerosols generated from the gas-to-particle conversion of pollutants are also a significant contributor of small particles at the mid latitudes of the northern hemisphere. Outflows over the oceans from the east coasts of the continents are characterized by a moderately large optical thickness and a large Ångström exponent indicating the effect of these industrial small particles.

In order to study the cloud-aerosol interaction phenomenon, the effective particle radius of the water cloud droplets, r_e, has been recognized as an important parameter. Han *et al*. (1994) showed a systematic reduction in the effective radius

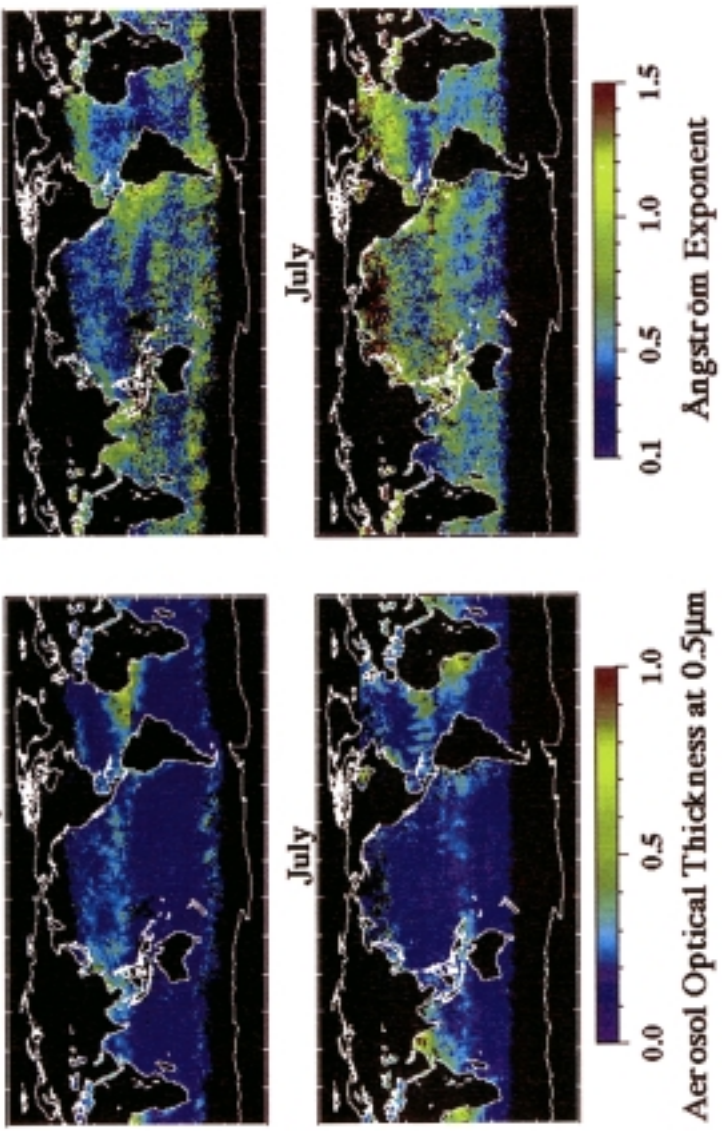

Fig. 1. Global distributions of aerosol optical thickness and Ångström exponent from AVHRR. Monthly means in January and July 1990 (Higurashi *et al.*, 2000)

of water cloud droplets retrieved from AVHRR and ISCCP cloud statistics. Wetzel and Stow (1999) found a negative correlation between τ_a and r_e after analyzing the long term data of AVHRR. Kawamoto *et al*. (2001) have developed an algorithm to simultaneously retrieve the cloud optical thickness and the effective particle radius from channel 1, 3 and 4 of AVHRR. They have shown that the effective particle radius has a characteristic land/ocean contrast and cloud top height dependence that can be consistently explained by the difference in the CCN concentration. It will be useful to utilize these remote sensing results for studying cloud-aerosol interaction phenomenon. As for in situ measurements, there have been many studies on the correlation between cloud particle number with CCN or aerosol number (Twomey *et al*., 1984; Martin *et al*., 1994; Andreae *et al*., 1995). Although it is difficult to directly obtain such a correlation from satellite remote sensing, Nakajima *et al*. (2001) argued for the method of estimating the columnar number of aerosol particles and cloud particles from the observed optical thickness and effective particle radius (or Ångström exponent for aerosol case). The evaluation is relatively accurate for the cloud case unless the cloud layer has significant drizzle particles and is given by the following relationship:

$$N_c = \frac{\tau_c}{2\pi r_e^2} e^{3\sigma^2}, \tag{2}$$

where σ is the log-dispersion of a log-normal size distribution of cloud polydispersion. On the other hand, the following product of the satellite observables is a good indicator of the column aerosol number:

$$N_a \propto \alpha\tau_a, \tag{3}$$

though the absolute value of N_a is difficult to estimate. Figure 2 shows the column number distributions thus obtained for aerosol and cloud from AVHRR data of four months (January, April, July, and October) in 1990 for latitudes less than 60°. In this analysis, water clouds are selected with the cloud top temperature greater than 273 K. It is found from the figure that there are similarities and differences in the distribution patterns. Both N_a and N_c are large over ocean areas adjacent to the continents, other than off California area where N_a is small and N_c. is large. Most of the tropical regions have a large N_a but small N_c. Therefore, Nakajima *et al*. (2001) have concluded there are three airmass types of different magnitudes in the cloud-aerosol interaction strength, i.e., strong (large N_a and N_c), vulnerable (small N_a and large N_c), and weak (large N_a and small N_c) regions.

Figure 3 shows a scatter plot between N_a and N_c for the results in Fig. 2 over the ocean. It is found that there is a good log-log linear correlation with the slope of about k = 0.5,

$$N_c = CN_a^k. \tag{4}$$

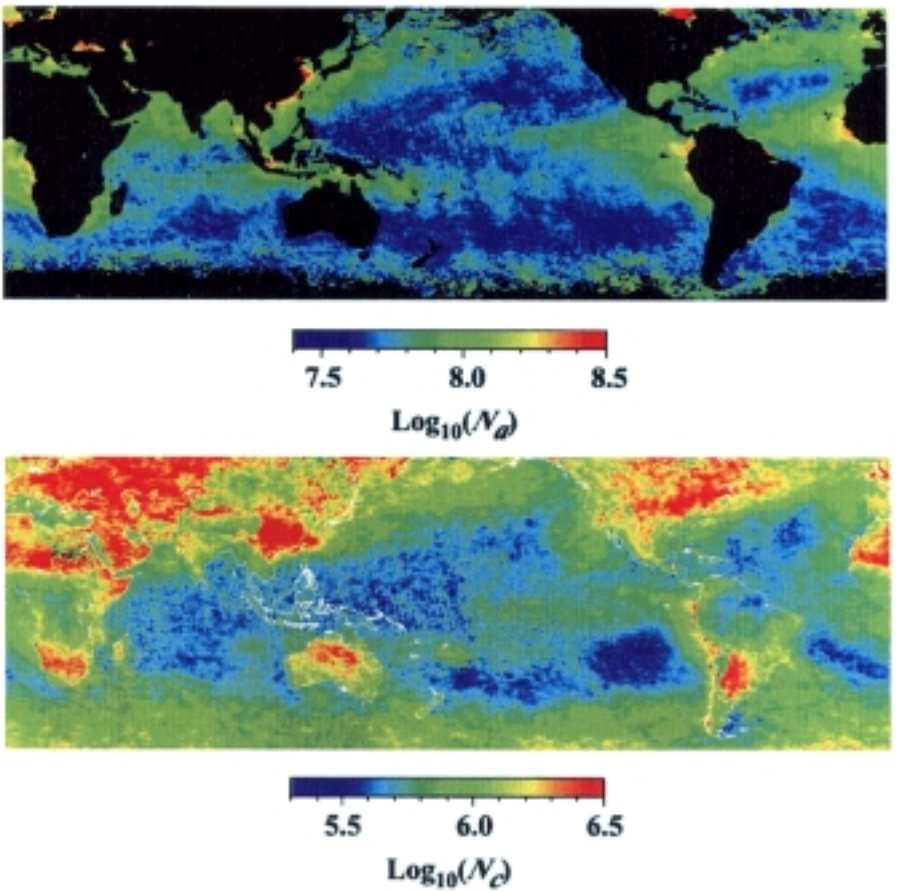

Fig. 2. Column number distributions of aerosol particles (N_a) and cloud particles (N_c) for four months (January, April, July, and October) in 1990 derived from AVHRR remote sensing (Nakajima *et al.*, 2001).

The exponent k of the above relation is smaller than the values 0.7–0.8 summarized by Kaufman *et al.* (1991), but larger than the proposed value of 0.26 by Jones *et al.* (1994).

EVALUATION OF THE RADIATIVE FORCING OF AEROSOLS

In order to make an accurate estimation of the radiative forcing due to the direct effect of anthropogenic aerosols, an accurate simulation of the global aerosol distribution is important. The recent trend in research is the direct simulation of the optical properties of aerosols by general circulation models coupled with aerosol chemical transport models. Takemura *et al.* (2000) successfully simulated the optical thickness of four types of aerosols, i.e., sulfate,

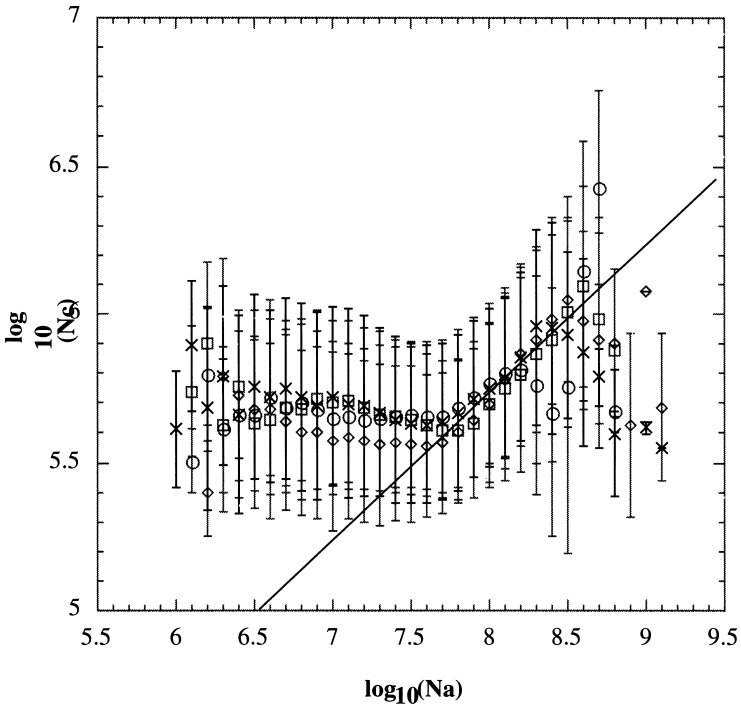

Fig. 3. Scatter plot between N_a and N_c for the data in Fig. 2 (Nakajima *et al*., 2001).

carbonaceous, soil dust, and sea salt aerosols. This simulated result can be directly compared with the observed values by AVHRR remote sensing and surface measurements by sky/sun-photometers. Figure 4 shows the latitudinal distribution of the aerosol optical thickness along the 22.5 W longitude in January 1990. The tropical Atlantic region along the longitude line is heavily loaded with Saharan dust aerosols. It is found, however, from the figure that it is difficult to explain the magnitude and location of the peak in the optical thickness around 10°N only by soil dust aerosol simulation. The figure clearly shows that the contribution of biomass burning aerosols from South Africa produces a comparable contribution to the atmospheric turbidity in the tropics. The particle radius of the biomass burning aerosols is typically 10 times smaller than that of dust aerosols, so that the small mass loading of biomass burning aerosols can produce a significant contribution of the optical thickness, and hence, can generate a large change in the radiative forcing.

Figure 5 shows the global distribution of the single scattering albedo obtained by Takemura *et al*. (2001). The unique point in this study is that they validated their model result by the optical thickness and single scattering albedo measured by optical methods from the surface, such as AERONET products (Dubovik *et al*., 2001). The figure shows that the single scattering albedo is not

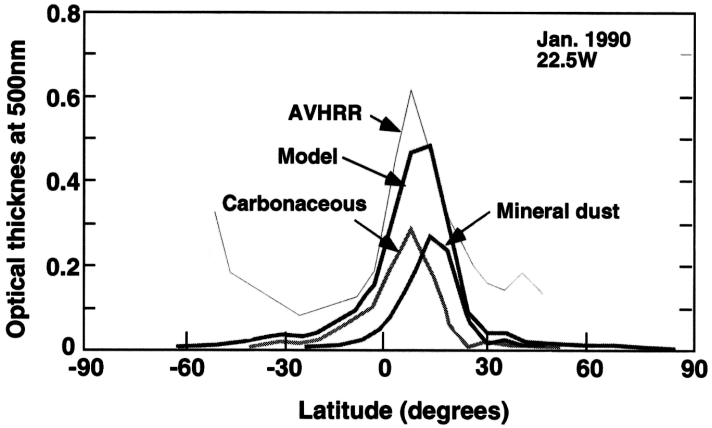

Fig. 4. Latitudinal dependence of the aerosol optical thickness along 22.5°W longitude line. Satellite value (AVHRR) and model simulation value (Model) are also shown with simulated contributions from mineral dust aerosols and carbonaceous aerosols (Takemura *et al.*, 2000).

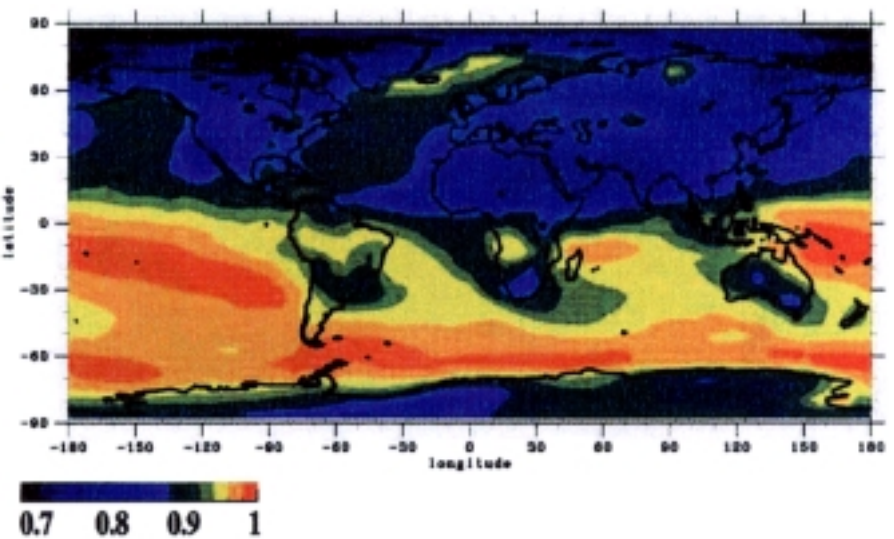

Fig. 5. Simulated global distribution of the single scattering albedo of aerosols. April 1990 case.

very close to 1 which was reported in the 1980's, but less than 0.9 in most of the northern hemisphere. It is found such a small single scattering albedo is spread over fairly large areas of the ocean and shows a distinct seasonal variation, indicating the long range transport of land-origin aerosols changing the optical properties of the remote maritime airmass. It is interesting to compare this feature

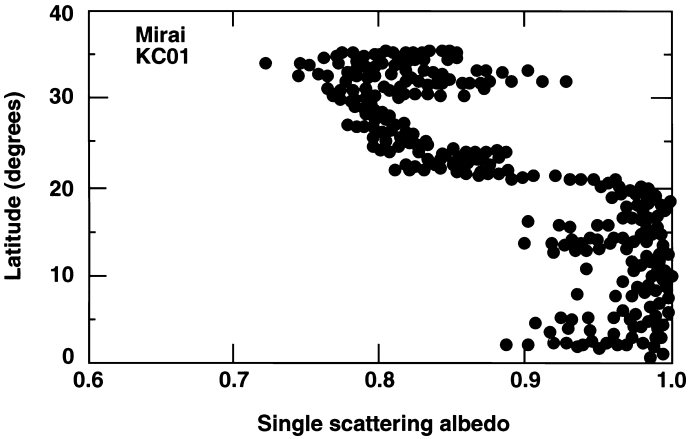

Fig. 6. Aerosol single scattering albedo along 140°E measured by MIRAI R/V. Data from the period of 8 February–10 March 1999. (Ohta *et al*., 2001).

with the measured single scattering albedo along the 140°E longitude line as in Fig. 6 that was measured on board the MIRAI research vessel by a nephelometer and aethelometer (Ohta *et al*., 2001) for the period from 8 February to 10 March 1999. The measured value shows that a small single scattering albedo was found as low as 0.8 in the region north of 20°N, which is consistent with the distribution shown in Fig. 5.

In conclusion, I added to Table 1 an estimate of the direct aerosol forcing by Takemura *et al*. (2001) and that of the indirect forcing by Nakajima *et al*. (2001). It is found that the total direct forcing is about –0.2 W/m^2 and much smaller than the other estimates in Table 1. Radiative forcing of black carbon aerosols is estimated to be +0.34 W/m^2 by Takemura *et al*. (2001) which entirely cancels the negative forcing by sulfate. It should be noted that the simulation of the aerosol optical properties by Takemura *et al*. (2001) has been validated by surface measurements of the aerosol optical thickness and single scattering albedo, so that the result is expected to be more accurate than the others. As for the radiative forcing of the indirect effect, Nakajima *et al*. (2001) obtained a rather wide range result from –0.7 W/m^2 to –1.7 W/m^2 over the ocean. They used, for the first time, a global satellite result of the correlation between N_a and N_c, so that their values can serve as an estimate independent of others. The total radiative forcing of aerosols is thus estimated in this study as –0.9 W/m^2 to –1.9 W/m^2 with a dominant contribution from the indirect effect more than the direct effect.

CONCLUSIONS

In this paper, we provided given some estimates of direct and indirect radiative forcing of aerosols from methods independent of the past studies. The total value is about –1.4 W/m^2 ± 0.5 W/m^2 which cancels about 60% of the

greenhouse gas warming. This value looks too large when the observed value of global warming is estimated as about 0.5 K until 1995 and the simulated warming without the aerosol effect is about 0.7 K (Mitchell *et al*., 1995; IPCC95, 1996). As understood in the present study, there are still significant error sources in the estimation, so that it is highly possible that the present estimate overestimated reality. Nonetheless, I dare to suggest there might be other warming sources to cancel this large aerosol cooling. In order to know which is reality, we need more studies in modeling/satellite remote sensing/in situ measurements.

REFERENCES

Andreae, M. O., W. Elbert, and S. J. de Mora, 1995: Biogenic sulfur emissions and aerosols over the tropical South Atlantic 3. Atmospheric dimethylsulfide, aerosols and cloud condensation nuclei, *J. Geophys. Res*., **100**, 11335–11356.

Charlson, R. J., S. E. Schwartz, J. M. Hales, R. D. Cess, J. A. Coakley, Jr., J. E. Hansen, and D. J. Hofmann, 1992: Climate forcing by anthropogenic aerosols, *Science*, **25**, 426–430.

Dubovik, O., B. N. Holben, T. F. Eck, A. Smirnov, Y. J. Kaufman, M. King, D. Tanré, and I. Slutsker, 2001: Climatology of aerosol absorption and optical properties in key locations, *J. Atmos. Sci*. (submitted).

Han, Q., W. B. Rossow, and A. A. Lacis, 1994: Near-global survey of effective droplet radii in liquid water clouds using ISCCP data, *J. Climate*, **7**, 465–497.

Hansen, J. E., M. Sato, A. Lacis, R. Ruedy, I. Tegen, and E. Matthews, 1998: Climate forcings in the industrial era, *Proc. Natl. Acad. Sci. USA*, **95**, 12753–12758.

Herman, J. R., P. K. Bhartia, O. Torres, C. Hsu, C. Seftor, and E. Celarier, 1997: Global distribution of UV-absorbing aerosols from Nimbus 7/TOMS data, *J. Geophys. Res*., **102**, 16911–16922.

Higurashi, A. and T. Nakajima, 1999: Development of a two channel aerosol retrieval algorithm on global scale using NOAA/AVHRR, *J. Atmos. Sci*., **56**, 924–941.

Higurashi, A., T. Nakajima, B. N. Holben, A. Smirnov, R. Frouin, and B. Chatenet, 2000: A study of global aerosol optical climatology with two channel AVHRR remote sensing, *J. Climate*, **13**, 2011–2027.

IPCC95, 1996: *Climate Change 1995, The Science of Climate Change*, edited by J. T. Houghton, L. G. Meira Filho, B. A. Callander, N. Harris, A. Kattenberg, and K. Maskell, Cambridge Univ. Press.

Jones, A., D. L. Roberts, and A. Slingo, 1994: A climate model study of indirect radiative forcing by anthropogenic sulphate aerosols, *Nature*, **370**, 450–453.

Kaufman, Y. J., R. S. Fraser, and R. L. Mahoney, 1991: Fossil fuel and biomass burning effect on climate, *J. Climate*, **4**, 578–588.

Kawamoto, K., T. Nakajima, and T. Y. Nakajima, 2001: A global determination of cloud microphysics with AVHRR remote sensing, *J. Climate*, **14**, 2054–2068.

Martin, G. M., D. W. Johnson, and A. Spice, 1994: The measurement and parameterization of effective radius of droplets in warm stratocumulus clouds, *J. Atmos. Sci*., **51**, 1823–1842.

Mitchell, J. F. B., T. C. Johns, J. M. Gregory, and S. F. B. Tett, 1995: Climate response to increasing levels of greenhouse gases and sulphate aerosols, *Nature*, **376**, 501–504.

Moulin, C., E. Lambert, F. Dulac, and U. Dayan, 1997: Control of atmospheric export of dust from North Africa by the North Atlantic Oscillation, *Nature*, **387**, 691–694.

Nakajima, T. and A. Higurashi, 1998: A use of two-channel radiances for an aerosol characterization from space, *Geophys. Res. Lett*., **25**, 3815–3818.

Nakajima, T., A. Higurashi, K. Kawamoto, and J. E. Penner, 2001: A possible correlation between satellite-derived cloud and aerosol microphysical parameters, *Geophys. Res. Lett*., **28**, 1171–1174.

Ohta, S., A. Ueda, T. Endoh, and S. Yamagata, 2001: Measurement of optical and chemical properties of atmospheric aerosols on the western Pacific Ocean in 1999 by research vessel

Mirai, *J. Global Environ. Eng.* (submitted).
Platnick, S., P. A. Durkee, K. Nielsen, J. P. Taylor, S.-C. Tsay, M. D. King, R. J. Ferek, P. V. Hobbs, and J. W. Rottman, 2000: The role of background cloud microphysics in the radiative formation of ship tracks, *J. Atmos. Sci.*, **57**, 2607–2624.
Rosenfeld, D., 2000: Suppression of rain and snow by urban and industrial air pollution, *Science*, **287**, 1793–1796.
Takemura, T., H. Okamoto, Y. Maruyama, A. Numaguti, A. Higurashi, and T. Nakajima, 2000: Global three-dimensional simulation of aerosol optical thickness distribution of various origins, *J. Geophys. Res.*, **105**, 17853–17873.
Takemura, T., T. Nakajima, O. Dubovik, B. N. Holben, and S. Kinne, 2001: Single scattering albedo and radiative forcing of various aerosol species with a global three-dimensional model, *J. Climate* (submitted).
Twomey, S., M. Piepgrass, and T. L. Wolfe, 1984: An assessment of the impact of pollution on global cloud albedo, *Tellus*, **36B**, 356–366.
Wetzel. A. and L. L. Stowe, 1999: Satellite-observed patterns in stratus microphysics, aerosol optical thickness, and shortwave radiative forcing, *J. Geophys. Res.*, **104**, 31287–31299.

T. Nakajima (e-mail: teruyuki@ccsr.u-tokyo.ac.jp), A. Higurashi, K. Kawamoto and T. Takemura